Supporting Information for

ORIGINAL ARTICLE

Broad-spectrum and powerful neutralization of bacterial toxins by erythroliposomes with the help of macrophage uptake and degradation

Chunying Liu[a], Shuangrong Ruan[b], Ying He[a], Xuejing Li[a], Yuefei Zhu[a, c], Honglan Wang[d], Hanwei Huang[a], Zhiqing Pang[a,*]

[a]*School of Pharmacy, Fudan University, Key Laboratory of Smart Drug Delivery, Ministry of Education, Shanghai 201203, China*

[b]*The Institute for Biomedical Engineering & Nano Science, Tongji University School of Medicine, Shanghai 200092, China*

[c]*Department of Biomedical Engineering, Columbia University, New York, NY 10027, USA*

[d]*Institute of Hematology, Union Hospital, Tongji Medical College, Huazhong University of Science & Technology, Wuhan, 430022, China*

Received 30 December 2021; received in revised form 14 January 2022; accepted 8 February 2022

*Corresponding authors. Tel./fax: +86 21 51980069.

E-mail address: zqpang@fudan.edu.cn (Zhiqing Pang).

1. Supporting methods

1.1. Dot blotting analysis of Hl*α* sponged with RM-PL

A dot blotting assay was performed to confirm the presence of Hlα on RM-PL+Hl*α* after the incubation of RM-PL and Hl*α*. Briefly, Hl*α* (2 μg) was incubated with RM-PL (10 μg) for 30 min, and then the mixture was spin down after ultracentrifugation (1,000,000 × *g*) for 120 min. The pellet was resuspended in water. Then the supernatant and the pellet (RM-PL+Hl*α*) were dotted on the nitrocellulose membrane, dried in air, probed with anti-Hl*α* antibody, and detected according routing

protocols. As a positive control, free Hl*α* with equal Hl*α* concentration to RM-PL+Hl*α* was tested in parallel.

1.2. Inflammatory cell assay after *in vivo* detoxification of PFTs by RM-PL following subcutaneous challenge

Six-week-old male ICR mice were randomly divided into three groups of nine mice (3 mice for each toxin). For the detoxification group, RM-PL was incubated with each toxin at the dose ratio of IC100 to HD100 for 30 min at room temperature, and the mixture was then injected subcutaneously into the hind legs of the mice. Mice received free toxins without RM-PL served as positive controls. For negative control, equal volume of PBS was injected. The injection site was photographed and the lesion area was recorded daily. At 3 days after injection, the mice were sacrificed, and the damaged skins and adjacent tissues were collected for flow cytometry analysis. Tissues were rinsed in PBS, cut into smaller pieces, rinsed into DPBS containing 1 mg/mL of Collagenase D, 0.1 mg/mL of DNase I, and 0.1 mg/mL of Dispase II, and incubated at 37 ℃ for 2 h. After incubation, undigested debris was removed by passing the sample through a 40-μm strainer. Cells were collected by centrifugation at 4 ℃ for 5 min at 500 × *g*, blocked with 1% (*w*/*v*) BSA and stained with APC-anti-CD45 (Biolegend, USA), Pacific blue-anti-CD11b (Biolegend, USA), FITC-anti-F4/80 (Biolegend, USA), PE-anti-Gr-1 (Biolegend, USA). Leukocytes, macrophages, monocytes, and neutrophils in each sample were sorted by BD FACS Aria II flow cytometer (BD Biosciences, USA). Data were analyzed using FlowJo software (Tree Star, USA).

1.3. Effect of RM-PL and RM-PL+Hlα on macrophage polarization

RAW 264.7 cells were seeded in 12-well plates at the density of 2×10^5 cells per well and cultured for 24 h. The cells were washed with PBS and subsequently treated with 0.8 mg/mL of RM-PL or RM-PL+Hl*α*. After 4 h incubation, the cells were harvested, washed with PBS and analyzed by flow cytometry (Beckman, CA, USA) after

staining with fluorescence-labeled antibodies against cell type specific markers ($CD80^+$ M1 phenotype, $CD86^+$ M1 phenotype and $CD206^+$ M2 phenotype).

2. Supporting figures

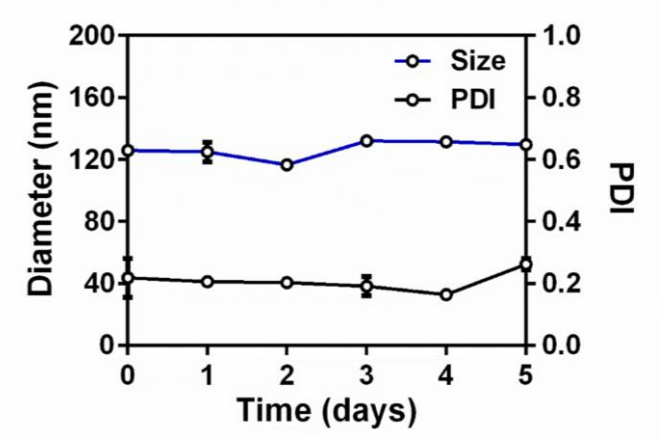

Figure S1 The stability of RM-PL in the PBS containing 5% FBS over 5 days (mean ± SD, n = 3).

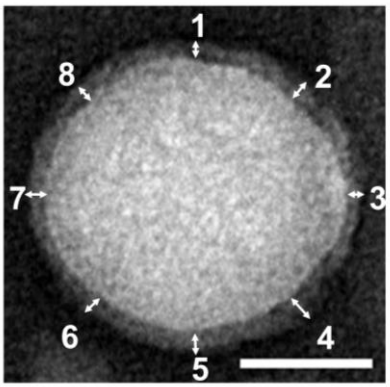

Number	Length (nm)
1	6.22
2	9.16
3	5.85
4	11.62
5	8.42
6	8.01
7	7.25
8	6.80
Average	**7.92**

Figure S2 Representative transmission electron microscopy (TEM) image of RM-PL (left) and the membrane width of RM-PL at different positions (right). Scale bar = 50 nm (white).

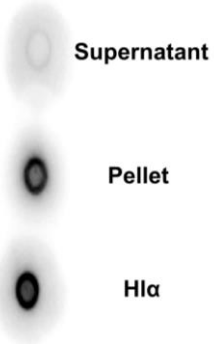

Figure S3 Dot blotting analysis of Hl*α* sponged with RM-PL after staining with anti-Hl*α* antibody. Hl*α* was incubated with RM-PL and then ultra-centrifuged. The supernatant and the pellet (RM-PL+Hl*α*) was analyzed by dot blotting. Free Hl*α* with equal Hl*α* concentration to RM-PL+Hl*α* was tested in parallel.

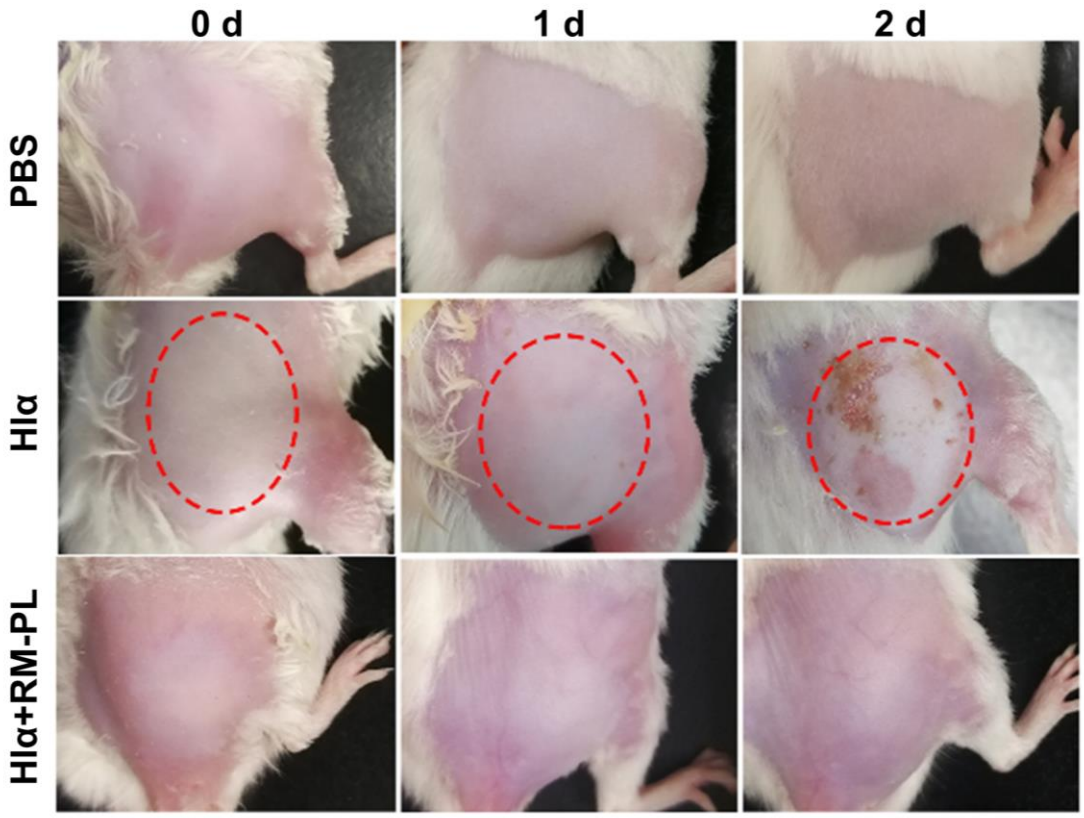

Figure S4 Skin images at different time points after the injection of PBS, Hl*α*, and Hl*α*+RM-PL. The red dotted circle indicated the lesion area.

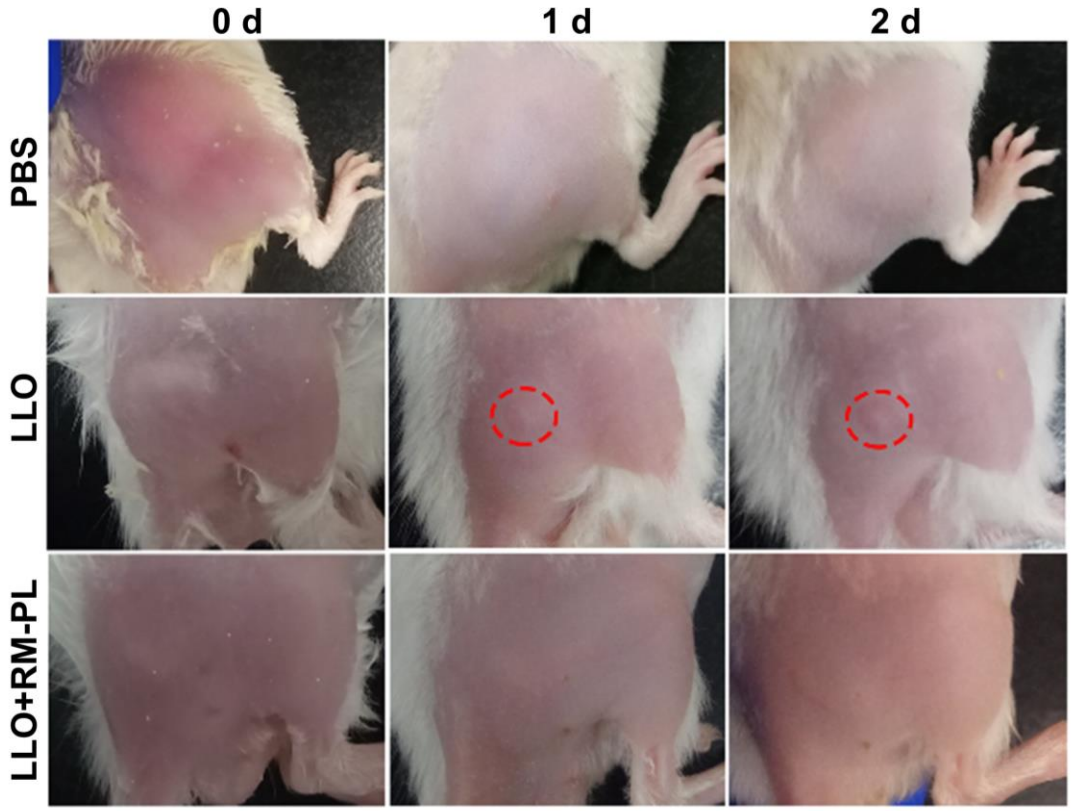

Figure S5 Skin images at different time points after the injection of PBS, LLO, and LLO+RM-PL. The red dotted circle indicated the lesion area.

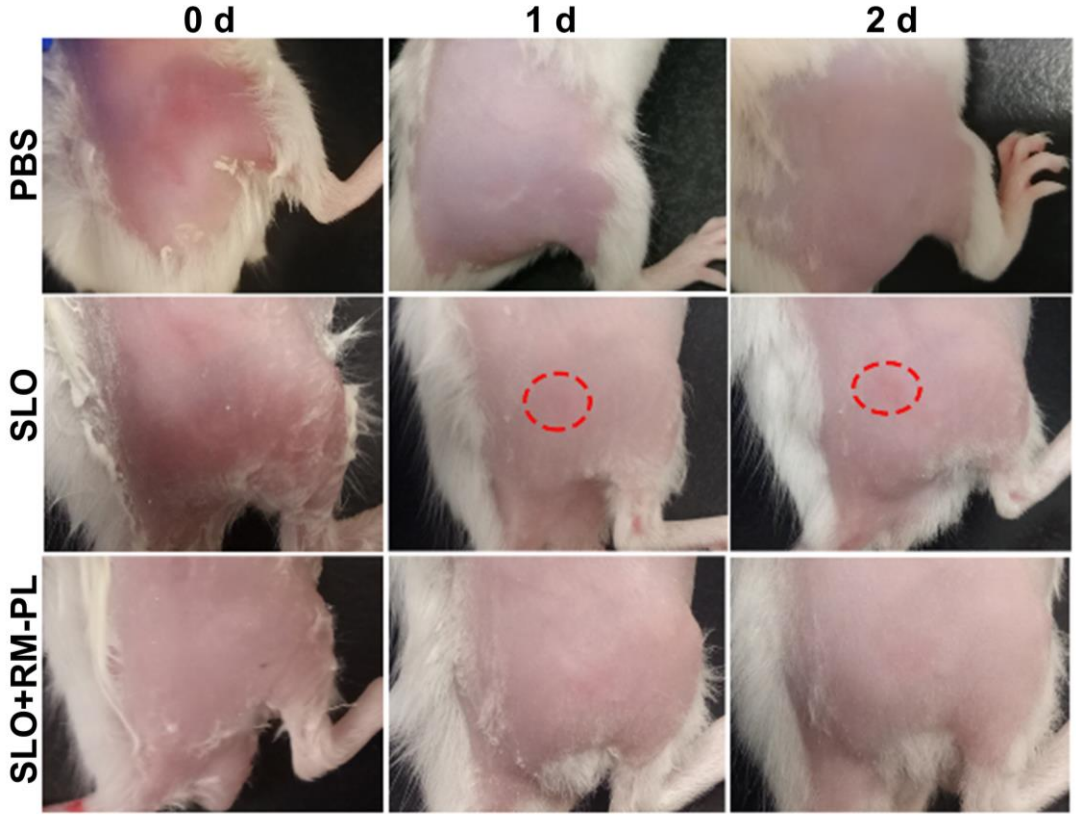

Figure S6 Skin images at different time points after the injection of PBS, SLO, and SLO+RM-PL. The red dotted circle indicated the lesion area.

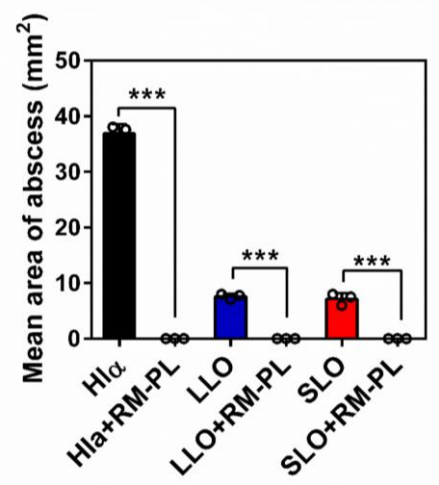

Figure S7 The mean skin lesion area of different treatment groups at 3 days after subcutaneous toxin challenge (mean ± SD, n=3). ***P < 0.001.

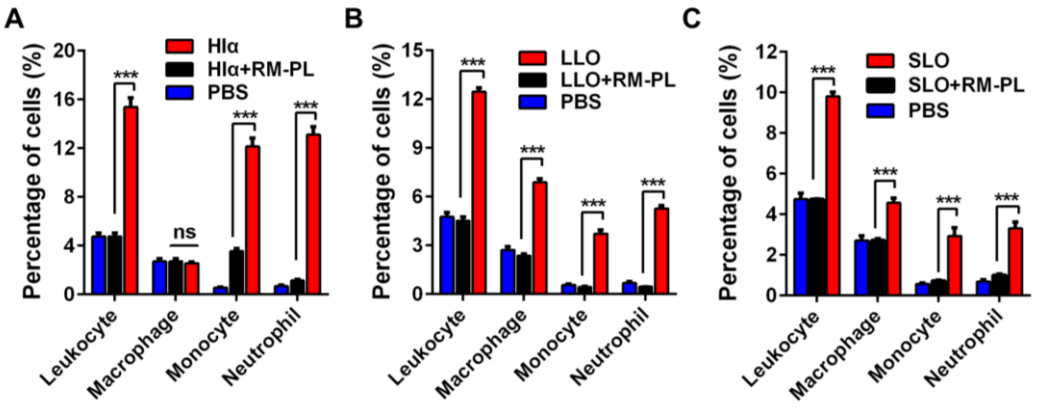

Figure S8 Percentage of inflammatory cells in damaged skins and adjacent tissues of ICR mice after subcutaneously injection of the mixture of toxins and RM-PL or PBS (mean ± SD, n=3). ***P < 0.001. "ns" indicated no significance between two groups.

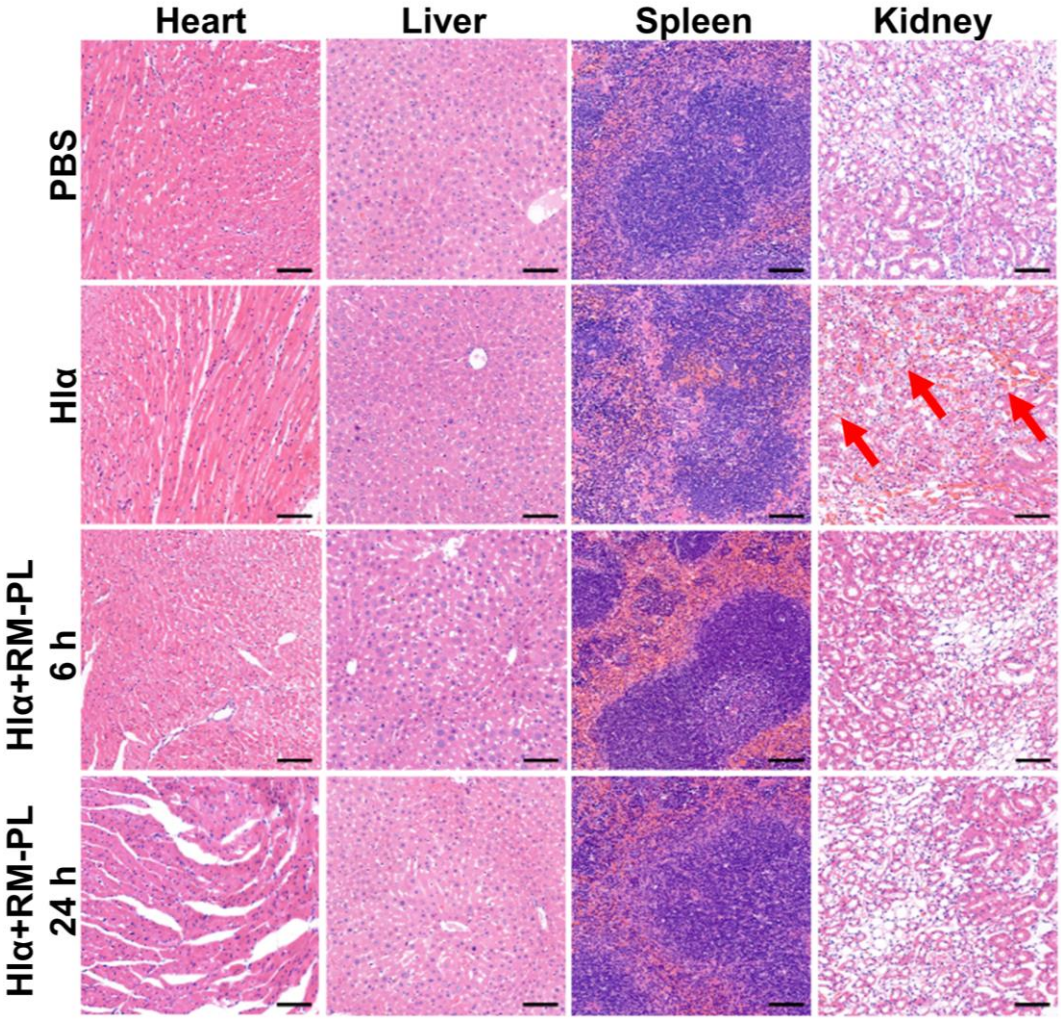

Figure S9 H&E staining of major organs after intravenous injection of PBS, Hlα, and Hlα+RM-PL. Scale bar = 50 μm.

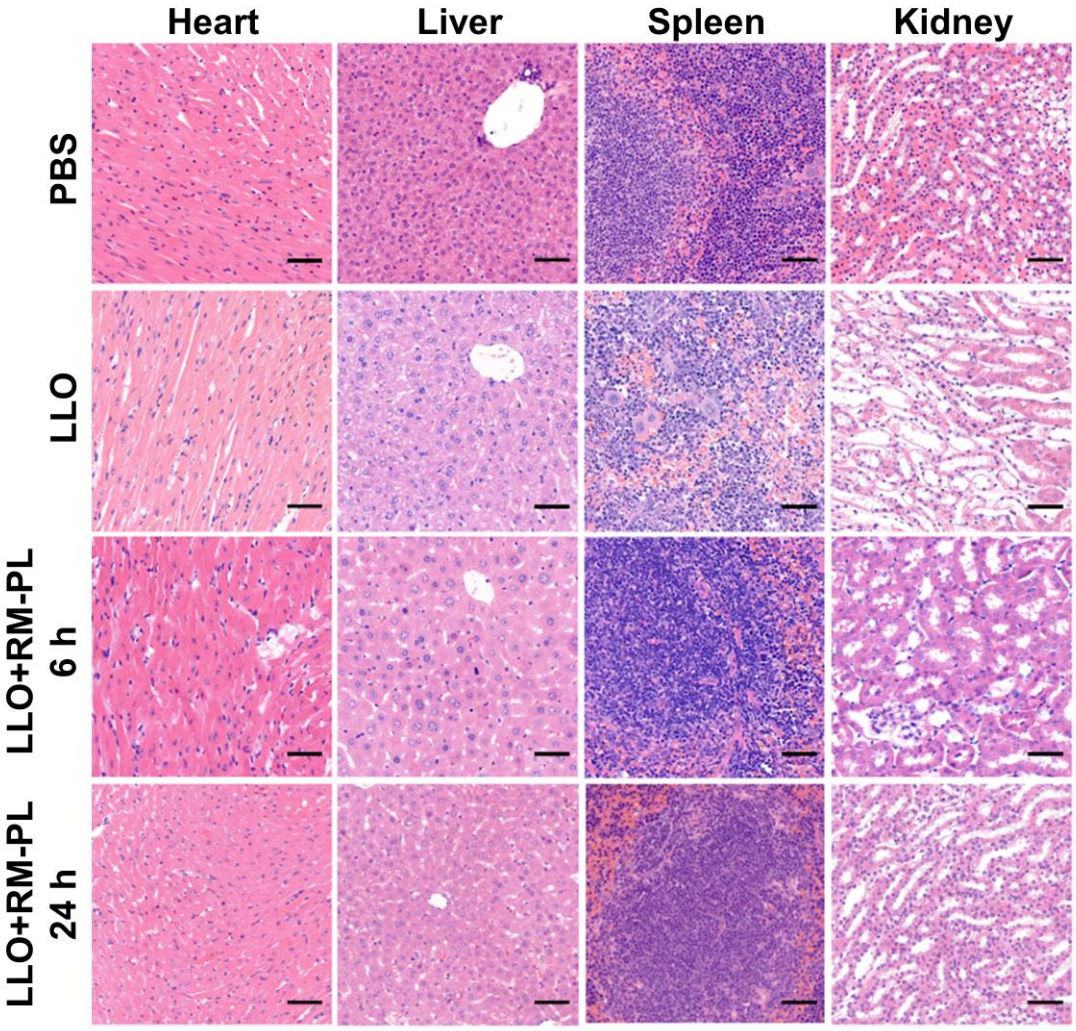

Figure S10 H&E staining of major organs after intravenous injection of PBS, LLO, and LLO+RM-PL. Scale bar = 50 μm.

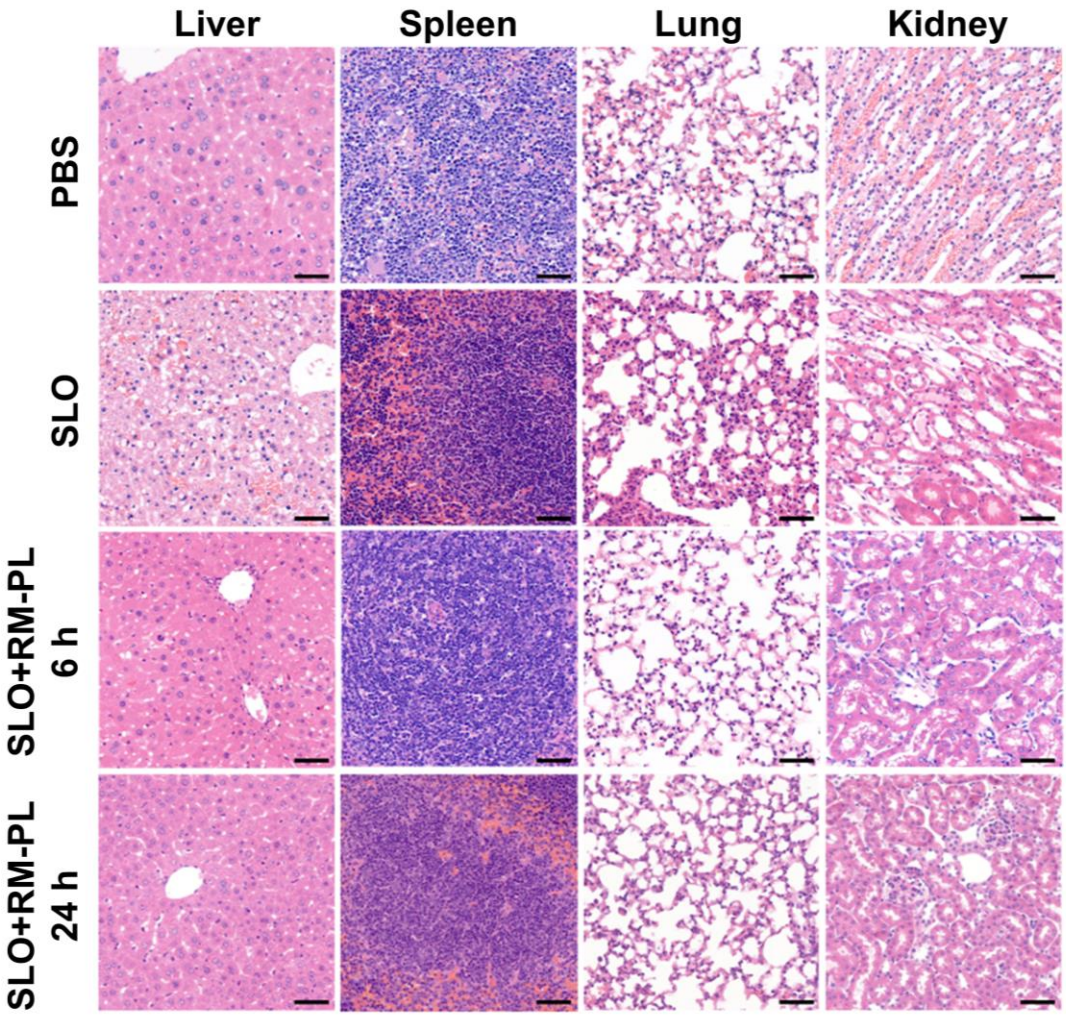

Figure S11 H&E staining of major organs after intravenous injection of PBS, SLO, and SLO+RM-PL. Scale bar = 50 μm.

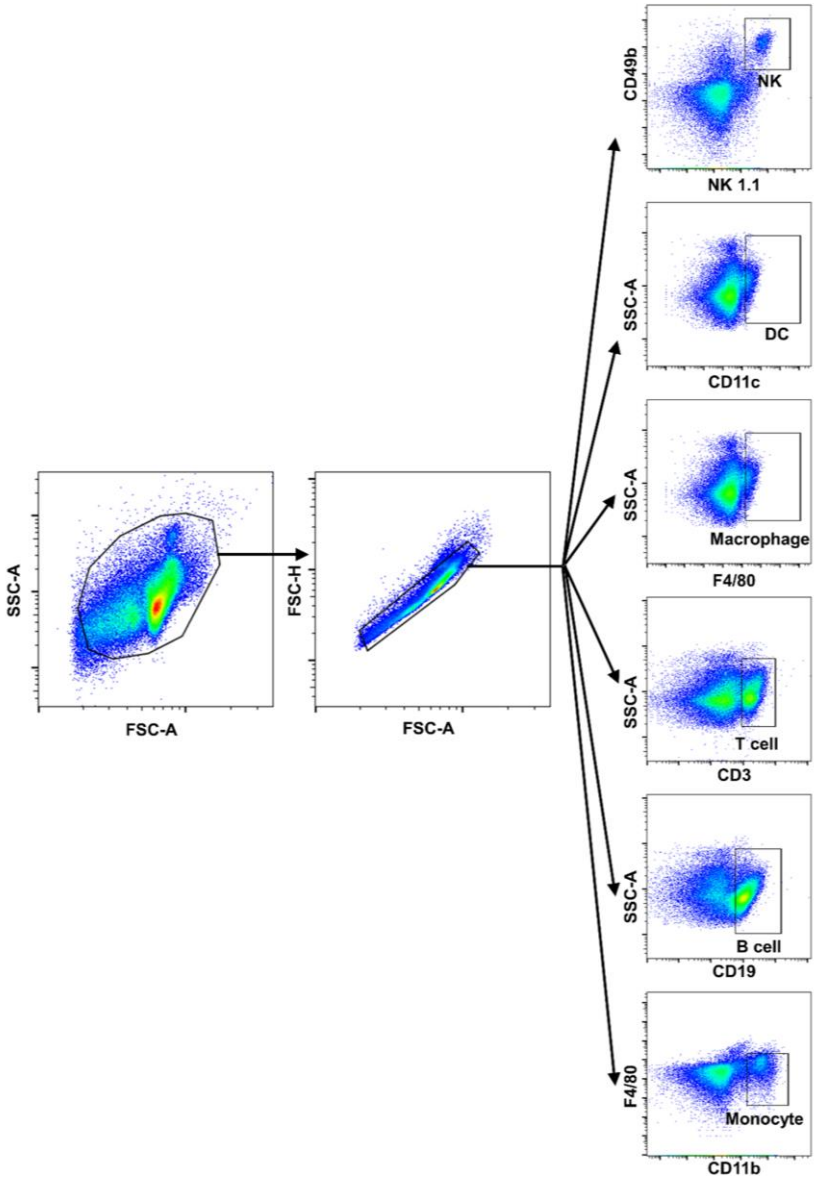

Figure S12 Gating strategy for ICR murine splenocytes. Viable cells were gated and then singlet cells were subdivided into $NK1.1^{+}CD49b^{+}$ NK cells, $CD11^{+}$ DC cells, $F4/80^{+}$ macrophages, $CD3^{+}$ T cell, $CD19^{+}$ B cells and $CD11b^{+}F4/80^{-}$ monocytes.

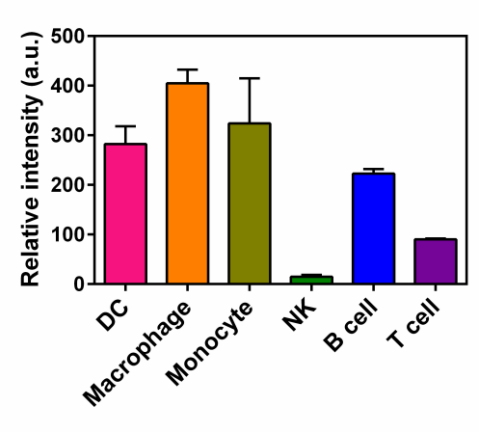

Figure S13 Quantitative summary of relative intensity of different cells in the spleen based on the mean fluorescence intensity and relative amounts of each cell type in the spleen (mean ± SD, *n*=4).

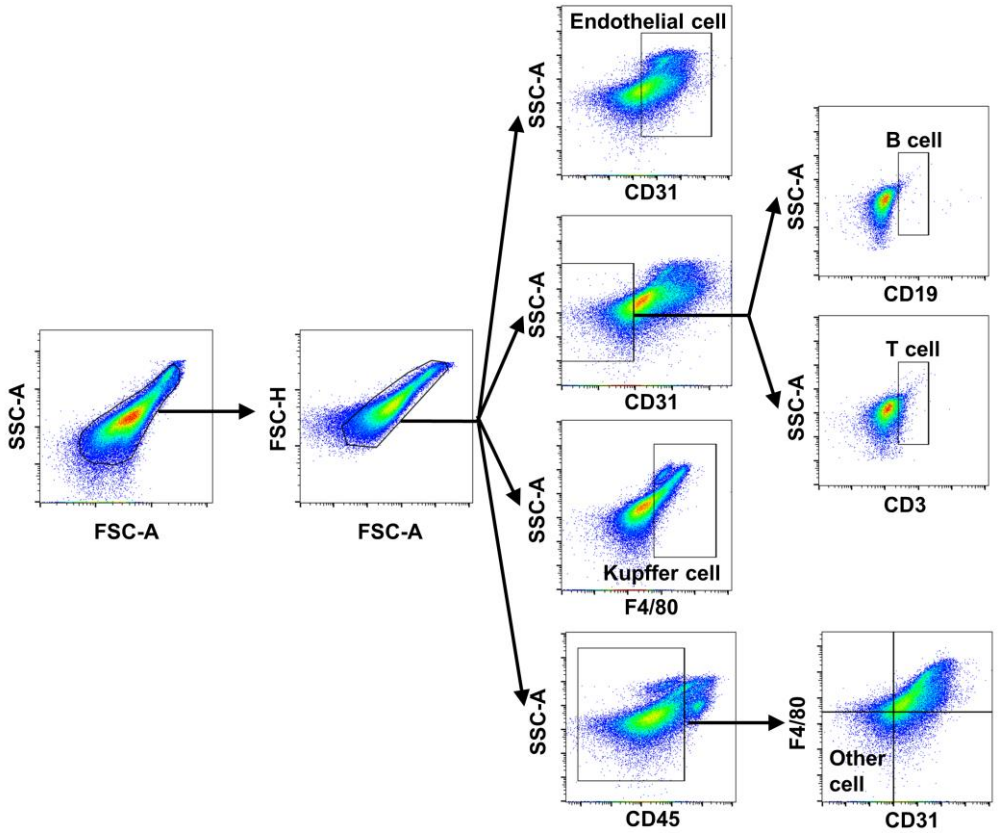

Figure S14 Gating strategy for ICR murine liver cells. Viable cells were gated and then singlet cells were subdivided into $CD31^+$ endothelial cells, $CD31^-CD19^+$ B cells, $CD31^-$CD3+ T cells, $F4/80^+$ Kupffer cells and $CD31^-F4/80^-CD45^-$ other cells.

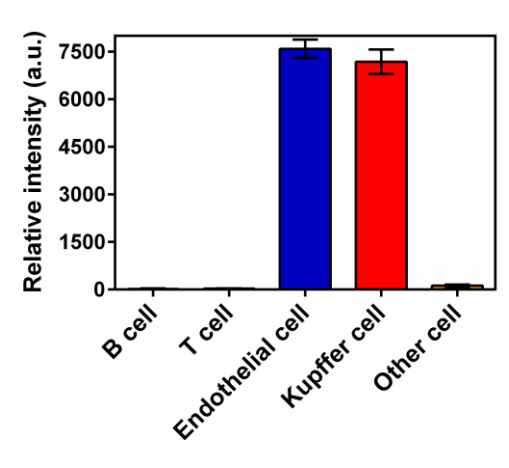

Figure S15 Quantitative summary of relative intensity of different cells in the liver based on the mean fluorescence intensity and relative amounts of each cell type in the liver (mean ± SD, *n*=4).

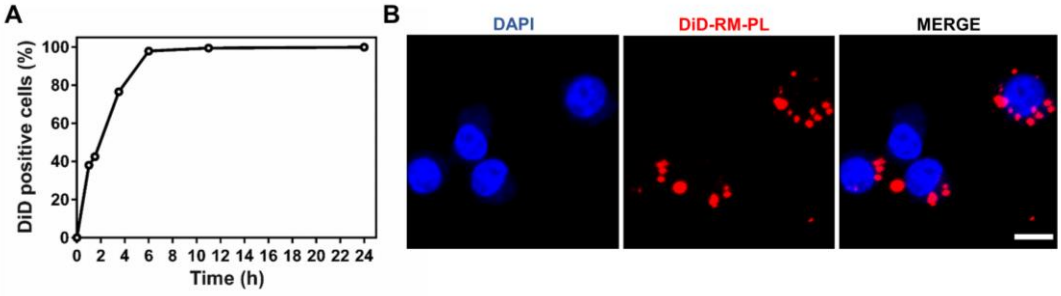

Figure S16 (A) Percentage of DiD-positive cells obtained by flow cytometry were plotted with time, demonstrating time-dependent cellular uptake profiles of DiD-labeled RM-PL+Hl*α* by RAW264.7 cells. (B) Representative fluorescence images of RAW 264.7 cells incubated with DiD-labeled RM-PL+Hl*α* for 4 h. Scale bar = 10 μm.

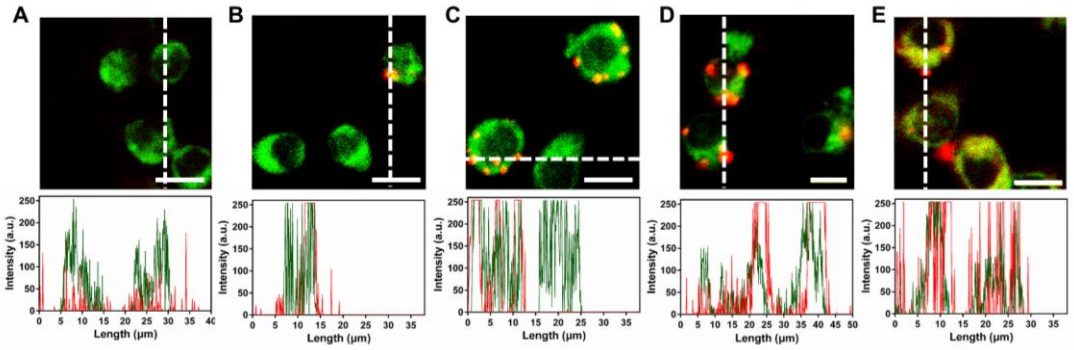

Figure S17 Confocal fluorescence microscopy images of RAW264.7 cells at different time points after incubation with DiD-labeled RM-PL+Hl*α* and the corresponding fluorescence intensity profiles of RM-PL (red) and lysosome (green) along the dotted white lines. (A) 0.5 h, (B) 2 h, (C) 4 h, (D) 6 h, and (E) 24 h. Scale bar = 10 μm.

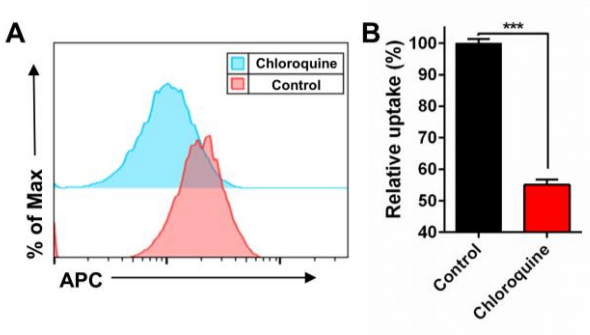

Figure S18 (A) Flow cytometry analysis and (B) the corresponding quantitative results for cellular uptake of DiD-labeled RM-PL+Hl*α* by RAW 264.7 cells in the presence of chloroquine (mean ± SD, *n*=3). Cells treated with DiD-labeled RM-PL+Hl*α* in the absence of chloroquine were used as Control. ****P* < 0.001.

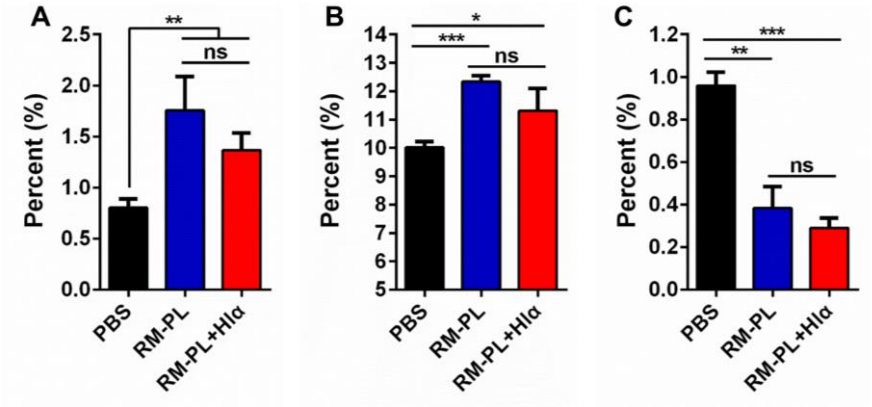

Figure S19 (A) CD80, (B) CD86 and (C) CD206 expression of RAW264.7 macrophages after incubation with RM-PL and RM-PL+Hl*α* (mean ± SD, *n*=3). **P* < 0.05, ***P* < 0.01, and ****P* < 0.001. "ns" indicated no significance between two groups.

3. Supporting tables

Table S1 Pharmacokinetic parameters of RM-PL absorbing Hlα in plasma (mean ± SD, n=4).

Group	MRT_{0-t} (h)	$MRT_{0-\infty}$ (h)	AUC_{0-t} (%ID/mL ħ)	$AUC_{0-\infty}$ (%ID/mL ħ)	CL (mL/h/kg)	$t_{1/2}$ (h)
RM-PL	8.9±0.1	18.5±1.4	1088±56	1511±118	0.005±0.001	13.2±1.2
RM-PL+Hlα	8.0±0.6*	12.9±3.2*	1027±312	1242±421	0.007±0.003	9.2±2.1*
RM-PL(Hlα)	7.8±0.2*	11.9±1.2*	1033±151	1203±150	0.007±0.001*	8.8±1.2*

MRT_{0-t}, mean residence time from time 0 to time t; $MRT_{0-\infty}$, mean residence time from 0 h to infinity; AUC_{0-t}, area under the concentration-time curve from time 0 to time t; $AUC_{0-\infty}$, area under the concentration-time curve from time 0 to infinity; CL, clearance; $t_{1/2}$, half-life. *P<0.05, compared with RM-PL.

4. Supporting discussion

4.1. Estimated surface area ration of lipid membranes to RBC membranes

Mass of PC: M = 758 g per mole

Mass of cholesterol: M = 387 g per mole

PC molecules for 2.0 mg of PC: 1.59×10^{18}

Cholesterol molecules for 1.6 mg of cholesterol: 2.49×10^{18}

Lipid molecules for a 100-nm liposome[1]: $\approx10^{5}$

Numbers of liposomes made of 2.0 mg of PC and 1.6 mg of cholesterol: 4.08×10^{13}

Surface area per liposome sized 100 nm: $4\pi R^2 = 3.14\times10^{-14}$ m^2

Total surface area of liposomes (S1): 1.28 m^2

Surface area per RBC[2]: ≈75 μm^2

RBC count in whole blood: ≈5 ×10^9 per mL

Total surface area of 150 μL of RBCs (S2): 0.056 m^2

Surface area ration of lipid membranes to RBC membranes: S1:S2 ≈ 23:1

4.2. Estimated Hl*α* neutralization capacity of RM-PL made from one single RBC

Based on the data in Figure 3F, 0.1 μg of RM-PL is able to neutralize 0.2 μg of *α*-hemolysin

4 mg of RM-PL (made of 150 μL of RBC membranes, 2.0 mg of PC, 1.6 mg of cholesterol, and 0.4 mg of DSPE-PEG) is able to neutralize 8.0 mg of *α*-hemolysin

Mass of *α*-hemolysin: M = 3.3×10^4 g per mole

Number (N1) of *α*-hemolysin molecule (8.0 mg): 1.46×10^{17}

RBC count in whole blood: ≈ 5×10^9 per mL

RBC number in 150 μL of RBCs (N2): 7.5×10^8

Hl*α* neutralization capacity of RM-PL made from one single RBC: N1/N2=1.95×10^8

Based on the data[2], one nanosponge (PLGA nanoparticles coated with RBC membranes) could neutralize 85 *α*-toxin (or Hl*α*), while the number of nanosponges made from a single RBC was approximately 3300. Hence, Hl*α* neutralization capacity of nanosponges made from one single RBC was 2.81×10^5.

Hl*α* neutralization capacity of RM-PL *versus* nanosponges made from one single RBC: ≈ 694:1

4.3. Estimated Hl*α* neutralization capacity per RM-PL

Numbers of liposomes made of 2.0 mg of PC, 1.6 mg of cholesterol: 4.08×10^{13}

Surface area ration of lipid membranes to RBC membranes: S1:S2=23:1

Numbers of RM-PL (N3) made of 150 μL of RBC membranes, 2.0 mg of PC, 1.6 mg of cholesterol, and 0.4 mg of DSPE-PEG: 4.25×10^{13}

Number (N1) of α-hemolysin molecule (8.0 mg): 1.46×10^{17}

Hlα neutralization capacity per RM-PL: N1/N3 ≈ 3430

4.4. Estimated SLO neutralization capacity of RM-PL made from one single RBC

Based on the data in Figure 3H, 1 μg of RM-PL is able to neutralize 0.3 μg of SLO

4 mg of RM-PL (made of 150 μL of RBC membranes, 2.0 mg of PC, 1.6 mg of cholesterol, and 0.4 mg of DSPE-PEG) is able to neutralize 1.2 mg of SLO

Mass of SLO: M = 6.3×10^{4} g per mole

Number (N4) of SLO molecule (1.2 mg): 1.15×10^{16}

RBC count in whole blood: ≈ 5×10^{9} per mL

RBC number in 150 μL of RBCs (N2): 7.5×10^{8}

SLO neutralization capacity of RM-PL made from one single RBC: N4/N2=1.53×10^{7}

Based on the data[2], one nanosponge (PLGA nanoparticles coated with RBC membranes) could neutralize 30 SLO, while the number of nanosponges made from a single RBC was approximately 3300. Hence, SLO neutralization capacity of nanosponges made from one single RBC was 9.9×10^{4}.

SLO neutralization capacity of RM-PL versus nanosponges made from one single RBC: ≈ 154:1

4.5. Estimated SLO neutralization capacity per RM-PL

Numbers of RM-PL (N3) made of 150 μL of RBC membranes, 2.0 mg of PC, 1.6 mg of cholesterol, and 0.4 mg of DSPE-PEG: 4.25×10^{13}

Number (N4) of SLO molecule (1.2 mg): 1.15×10^{16}

SLO neutralization capacity per RM-PL: N4/N3 ≈ 269

4.6. Estimated LLO neutralization capacity of RM-PL made from one single RBC

Based on the data in Figure 3G, 1 μg of RM-PL is able to neutralize 0.3 μg of LLO

4 mg of RM-PL (made of 150 μL of RBC membranes, 2.0 mg of PC, 1.6 mg of cholesterol, and 0.4 mg of DSPE-PEG) is able to neutralize 1.2 mg of LLO

Mass of LLO: M = 5.25×10^{4} g per mole

Number (N5) of LLO molecule (1.2 mg): 1.38×10^{16}

RBC count in whole blood: ≈ 5×10^{9} per mL

RBC number in 150 μL of RBCs (N2): 7.5×10^{8}

LLO neutralization capacity of RM-PL made from one single RBC: N5/N2=1.84×10^{7}

4.7. Estimated LLO neutralization capacity per RM-PL

Numbers of RM-PL (N3) made of 150 μL of RBC membranes, 2.0 mg of PC, 1.6 mg of cholesterol, and 0.4 mg of DSPE-PEG: 4.25×10^{13}

Number (N5) of LLO molecule (1.2 mg): 1.38×10^{16}

LLO neutralization capacity per RM-PL: N5/N3 ≈ 325

Supporting references

1 He Y, Li R, Li H, Zhang S, Dai W, Wu Q, et al. Erythroliposomes: integrated hybrid nanovesicles composed of erythrocyte membranes and artificial lipid membranes for pore-forming toxin clearance. *ACS Nano* 2019; **13**: 4148-59.

2 Hu CM, Fang RH, Copp J, Luk BT, Zhang L. A biomimetic nanosponge that absorbs pore-forming toxins. *Nat Nanotechnol* 2013; **8**: 336-40.